

Measurement of cross-relaxation times in $Tm^{2+}:SrF_2$ by optical means

T. Kohmoto

Department of Physics, College of Liberal Arts, Kyoto University, Sakyo-ku, Kyoto 606, Japan

Y. Fukuda

Department of Physics, College of Liberal Arts, Kobe University, Nada-ku, Kobe 657, Japan

T. Hashi

Department of Physics, Faculty of Science, Kyoto University, Sakyo-ku, Kyoto 606, Japan

(Received 31 October 1988)

Cross-relaxation times in $Tm^{2+}:SrF_2$ (0.02 at. % Tm^{2+}) were measured in low magnetic fields by optical means. The population difference in the ground state is created by optical pumping with a pulse laser, and its relaxation is monitored with a cw laser. The cross-relaxation times for the two-spin process, which cannot be measured by ESR techniques, were measured, as well as those for the three-spin process. The result was analyzed by using rate equations.

I. INTRODUCTION

Cross relaxation is an important mechanism for establishing spin thermal equilibrium in solids. In a previous paper,¹ we reported anomalous behavior of the optically detected ESR signals in $Tm^{2+}:SrF_2$ due to cross relaxation. However, the direct measurement of the cross-relaxation time has not been made in this system.

Cross relaxation has been studied by various techniques, for example, pulsed magnetic resonance,²⁻⁴ cw magnetic resonance,⁵ and ac magnetic susceptibility.^{6,7} The measurement of ac magnetic susceptibility is a useful technique. The crossing magnetic field can be determined, but it is an indirect method for the measurement of the cross-relaxation time. The direct measurement of the cross-relaxation time has been made by using a magnetic resonance method. A high-power pulsed microwave is applied to disturb the spin level population in high magnetic fields. The return to equilibrium is monitored with a low-power cw microwave. Cross relaxations for the three-spin process in ruby were examined in detail by using this method.³ The cross-relaxation time for the two-spin process, however, cannot be measured by this technique at the center of the crossing field, because the total population difference is not changed in this process. The time resolution is limited by the microwave pulse width and the dead time of the detector.

In this paper we report on an optical measurement of the cross-relaxation time in $Tm^{2+}:SrF_2$. Advantages of our optical technique are as follows. The cross-relaxation time is directly measured. Very fast relaxation time (up to about 10 nsec) can be observed. Not only three-spin processes but also two-spin processes can be investigated even at the center of the crossing field. The sensitivity is high enough even at low magnetic fields where population differences in thermal equilibrium is small.

In our experiment optical pumping with a circularly polarized light pulse creates population differences in the ground state through preferential depopulation due to the

circular dichroism of the optical transition. The relaxation of the magnetization after the pulsed excitation is optically monitored with a cw laser and a polarimeter. The optical pumping creates a large population difference even in low magnetic fields where the thermal-equilibrium population difference is small, and the time resolution is determined by the pulse width of the pumping light. We obtained detailed information on the cross relaxation both for the two-spin as well as the three-spin processes.

The optical and magnetic properties of Tm^{2+} in SrF_2 are briefly summarized in Ref. 1. Electric dipole transitions from the ground state ($4f^{13}$) to the excited state ($4f^{12}5d$) form a broad absorption band in the visible region. The circular dichroism and the Faraday rotation of the optical transition are used to create and detect the magnetization. The spin Hamiltonian of the ground state in the magnetic field H is written as

$$\mathcal{H} = g\mu_B S \cdot H + AS \cdot I, \tag{1}$$

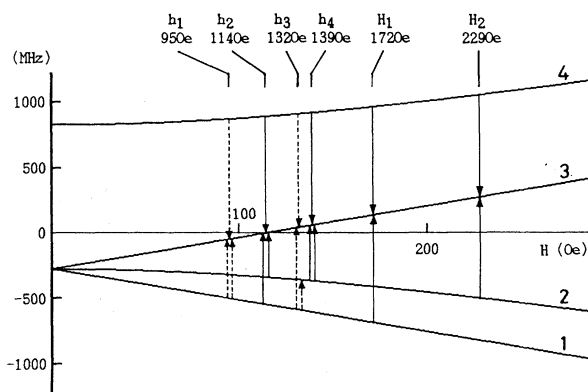


FIG. 1. Energy-level diagram and the expected cross-relaxation processes in the ground state of $Tm^{2+}:SrF_2$ below 300 Oe. The four processes indicated by solid lines are observed in our experiment.

TABLE I. Cross-relaxation processes expected in the ground state of $\text{Tm}^{2+}:\text{SrF}_2$. Three-spin processes are expected at h_i , and two- and three-spin processes at H_i .

	Magnetic field H Unit of $ A/g\mu_B $	(Oe)	Process
h_1	5/12	95.3	$2E_{13}=E_{34}$
h_2	1/2	114.3	$E_{13}+E_{23}=E_{34}$
h_3	$1/\sqrt{3}$	132.0	$E_{12}+E_{13}=E_{34}, 2E_{13}=E_{24}$
h_4	$(9-\sqrt{17})/8$	139.4	$2E_{23}=E_{34}$
H_1	3/4	171.5	$E_{13}=E_{34},$ $E_{12}+E_{23}=E_{34}, E_{13}+E_{23}=E_{24},$ $2E_{12}=E_{23}, 2E_{13}=E_{14}, 2E_{34}=E_{14}$
H_2	1	228.7	$E_{23}=E_{34},$ $E_{12}+E_{34}=E_{13}, E_{13}+E_{23}=E_{14},$ $2E_{23}=E_{24}, 2E_{34}=E_{24}$
h_5	4/3	304.9	$E_{12}+E_{13}=E_{24}, E_{12}+E_{34}=E_{23},$ $2E_{12}=E_{34}, 2E_{23}=E_{14}, 2E_{34}=E_{13}$
h_6	$(9+\sqrt{17})/8$	375.1	$2E_{34}=E_{23}$

with effective electron spin $S = \frac{1}{2}$ and Tm nuclear spin $I = \frac{1}{2}$. The energy eigenvalues ($E_i, i=1,2,3,4$) are obtained from Hamiltonian (1), and the energy-level diagram in low magnetic fields is shown in Fig. 1. Table I shows all possible two- ($E_{ij}=E_{kl}$) and three- ($E_{ij}+E_{kl}=E_{mn}$) spin processes and the cross-relaxation fields^{7,8} expected in the ground state, where $E_{ij}=E_j-E_i$. The spin processes expected below 300 Oe are schematically shown in Fig. 1. (Three-spin processes at H_1 and H_2 are not shown.) We observed cross relaxation shown by solid lines in Fig. 1 and analyzed these processes using rate equations.

II. EXPERIMENT AND RESULTS

The experimental setup is schematically shown in Fig. 2(a). The pump and probe lights are provided by a nitrogen-laser-pumped dye laser (5800 Å, 3 nsec, 10 kW) and a He-Ne laser (6328 Å, 1 mW), respectively. The pump (circularly polarized) and probe (linearly polarized) beams are nearly collinear (parallel to the [111] axis) and focused on the sample (0.02 at. % Tm^{2+} , 2 mm in thickness), which is in contact with a copper block at liquid-helium temperature. The waist sizes of the beams at the focus are about 100 μm . A static magnetic field up to 400 Oe is applied along the [111] axis. The magnetization parallel to the magnetic field is induced in the ground state by the pump pulse, and the decay of the induced magnetization is monitored as the change of the Faraday rotation of the probe light. The Faraday rotation is detected by a polarimeter. A Glan prism and two photodiodes are used in the polarimeter as shown in Fig. 2(b). The Faraday rotation angle is proportional to the magnetization, and the polarimeter output linearly responds to the Faraday rotation angle when it is small.¹

Figure 3 shows the Faraday rotation signals around H_2

(~ 229 Oe) where one of the two-spin processes occurs. The pump pulse excites the sample at $t=0$, and the repetition rate is 4 Hz. The fast decay of the magnetization around 229 Oe is due to the cross relaxation, and the cross-relaxation time at the center of the crossing field is 36 μsec under the approximation of the exponential decay. A slight inclination of the background comes from the ac coupling of the amplifier. The decay due to the spin-lattice relaxation is much slower.

Similar curves were observed around $H_1, h_4,$ and h_2 (< 200 Oe), and the cross-relaxation rates (the inverse of the observed decay times) obtained from the Faraday ro-

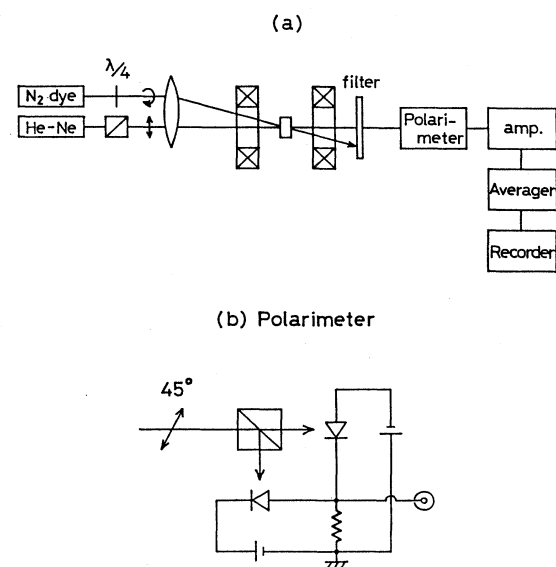


FIG. 2. (a) Experimental setup for the measurement of the cross-relaxation time and (b) construction of the polarimeter.

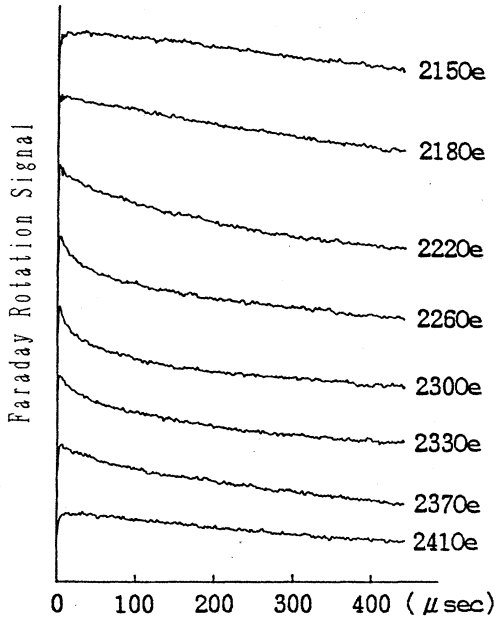


FIG. 3. Time evolution of the Faraday rotation signals around $H_2 = 229$ Oe after the pump light pulse at $t = 0$.

tation signals are potted in Fig. 4. The observed Faraday rotation signals at the crossing fields were sums of several exponentials whose characteristic times were different. The fast decay components are due to the cross relaxation, and the slow ones are due to the spin-lattice relaxation. In our experimental condition two decay components due to

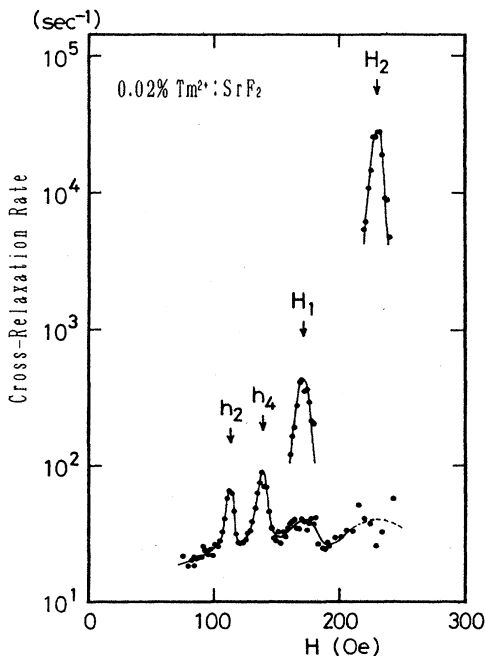


FIG. 4. Cross-relaxation rates (the inverse of the observed decay times) obtained from the Faraday rotation signals in low magnetic fields.

spin-lattice relaxation whose decay times are ~ 0.1 and ~ 0.5 sec were observed, which is independent of the magnetic field below 300 Oe. There are four distinct peaks in Fig. 4. The two peaks at the lower fields (h_2 and h_4) are due to the three-spin process, and the two peaks at the higher fields (H_1 and H_2) are due to the two-spin process. The cross-relaxation time τ_1 at each peak is as follows:

$$\begin{aligned} \tau_1(h_2) &= 15 \text{ msec}, & \tau_1(h_4) &= 11 \text{ msec}, \\ \tau_1(H_1) &= 2.3 \text{ msec}, & \tau_1(H_2) &= 36 \text{ } \mu\text{sec}. \end{aligned} \quad (2)$$

We examined the Faraday rotation signal up to 400 Oe, but the three-spin processes at h_1 , h_3 , h_5 , and h_6 were not observed. It is probably because their cross-relaxation times are longer than the spin-lattice relaxation time.

The changes of the signal amplitude due to the cross relaxations are $\sim 70\%$ (h_2), $\sim 60\%$ (h_4), $\sim 30\%$ (H_1), and $\sim 10\%$ (H_2) of the total Faraday rotation signal. When the magnetic field is shifted from the center of the crossing field, the decay time becomes longer and also the change of the signal amplitude becomes smaller. Two important factors, decay time and the amount of change involved in the cross relaxation, have been measured independently by our optical pulse method.

III. ANALYSIS BY RATE EQUATIONS

We analyze the observed cross relaxation using rate equations following Bloembergen *et al.*⁹ and Grant.¹⁰ The rate equations for $t > 0$ are written as

$$\frac{dn_i}{dt} = \sum_j (-r_{ij}n_i + r_{ji}n_j) + F_i + \frac{1}{4\tau}n^*, \quad (3)$$

$$\frac{dn^*}{dt} = -\frac{1}{\tau}n^*,$$

where n_i ($i = 1, 2, 3, 4$) is the population in the i th level in the ground state, n^* is the population in the excited state, r_{ij} ($i, j = 1, 2, 3, 4$) is the decay rate from the i th level to the j th level through the spin-lattice relaxation, τ is the lifetime of the excited state, and F_i is the term representing the cross relaxation.

We first consider the two-spin process at H_1 . The cross-relaxation terms for this process are written as

$$\begin{aligned} F_1 &= F_4 = -W(n_1n_4 - n_3^2), & F_2 &= 0, \\ F_3 &= 2W(n_1n_4 - n_3^2), \end{aligned} \quad (4)$$

where W is the cross-relaxation rate. These terms are nonlinear in n_i . However, Eqs. (3) and (4) can be linearized by considering our experimental conditions, that (1) energy differences in the ground state are much smaller than kT ($E_{ij} \ll kT$) and (2) population changes at the optical pumping are small enough ($|\Delta n_i|, |\Delta n^*| \ll 1$, weak pumping). To simplify the solution we assume that all spin-lattice relaxation rates are equal in the ground state ($r_{ij} = r$). This assumption is reasonable as long as the cross-relaxation rate is much larger than the spin-lattice relaxation rate. The time evolution $n_i(t)$ is thus obtained

TABLE II. The observed cross-relaxation times τ_1 and the cross-relaxation rates W determined by using rate equations.

	H (Oe)	Process	τ_1 (msec)	$1/\tau_1$ (sec $^{-1}$)	W (sec $^{-1}$)
h_2	114	$E_{13} + E_{23} = E_{34}$	15	6.7×10^1	7.6×10^1
h_4	139	$2E_{23} = E_{34}$	11	9.1×10^1	9.2×10^1
H_1	172	$E_{13} = E_{34}$	2.3	4.3×10^2	2.8×10^2
H_2	229	$E_{23} = E_{34}$	0.036	2.8×10^4	1.9×10^4

as

$$n_i(t) = A_i + B_i \exp(-t/\tau) + C_i \exp(-t/\tau_1) + D_i \exp(-t/\tau_2), \quad (5)$$

$$\frac{1}{\tau_1} = \frac{3}{2}W + 4r, \quad \frac{1}{\tau_2} = 4r, \quad (6)$$

where A_i , B_i , C_i , and D_i are constants, and τ_1 represents the observed cross-relaxation time and τ_2 the spin-lattice relaxation time. For the discussion of the two-spin process at H_2 the same rate equations (3) and (4) where subscripts 1 and 2 are interchanged can be used. The relaxation rates are given by the same expression as Eqs. (6).

Next we consider the three-spin processes. The cross-relaxation terms at h_2 are written as

$$F_1 = F_2 = F_4 = -W(n_1 n_2 n_4 - n_3^3), \quad (7)$$

$$F_3 = 3W(n_1 n_2 n_4 - n_3^3).$$

The rate equations are linearized in a similar way as in the two-spin process, and $n_i(t)$ can be written in the same form as in Eq. (5). But the expressions of relaxation rates are

$$\frac{1}{\tau_1} = \frac{3}{4}W + 4r, \quad \frac{1}{\tau_2} = 4r, \quad (8)$$

which are different from Eq. (6). For the three-spin process at h_4 we obtain

$$F_1 = 0, \quad F_2 = -2W(n_2^2 n_4 - n_3^3), \quad (9)$$

$$F_3 = 3W(n_2^2 n_4 - n_3^3), \quad F_4 = -W(n_2^2 n_4 - n_3^3),$$

and

$$\frac{1}{\tau_1} = \frac{7}{8}W + 4r, \quad \frac{1}{\tau_2} = 4r. \quad (10)$$

The results are summarized in Table II. The cross-relaxation rate W is obtained from the observed decay time τ_1 by using Eqs. (6), (8), and (10), and $4r = 10 \text{ sec}^{-1}$. The cross-relaxation rates for the two-spin processes are larger than those for the three-spin processes. As for the two-spin processes, the cross-relaxation rate at H_1 is much smaller than that at H_2 . This is because transition 1-3 involved in the former is forbidden, whereas two transitions involved in the latter are allowed.

IV. SUMMARY

We observed the cross relaxation in the ground state of $\text{Tm}^{2+}:\text{SrF}_2$ (0.02 at. % Tm^{2+}) by optical means in low magnetic fields. The circular dichroism and the Faraday rotation of the optical transition are responsible for the creation and detection of the magnetization. The cross-relaxation times were measured both for two- and three-spin processes. Since the time resolution is determined by the pulse width of the pumping light, it is expected that this method enables us to observe very fast relaxations.¹¹

The analysis of the cross relaxation was made by using rate equations. The nonlinear rate equations were linearized under some assumptions, and the cross-relaxation rates were determined from the experimental results.

¹T. Kohmoto, Y. Fukuda, and T. Hashi, Phys. Rev. B **34**, 6085 (1986).

²P. S. Pershan, Phys. Rev. **117**, 109 (1960).

³W. B. Mims and J. D. McGee, Phys. Rev. **119**, 1233 (1960).

⁴S. Y. Feng and N. Bloembergen, Phys. Rev. **130**, 531 (1963).

⁵P. T. Squire, Proc. Phys. Soc. London **86**, 573 (1965).

⁶R. Cremer, Phys. Status Solidi **42**, 507 (1970).

⁷E. B. Aleksandrov and V. S. Sapasskii, Fiz. Tverd. Tela (Leningrad) **20**, 1180 (1978) [Sov. Phys. Solid State **20**, 679 (1978)].

⁸M. Mitsunaga, Ph.D. thesis, University of California, Berkeley, 1983 (unpublished).

⁹N. Bloembergen, S. Shapiro, P. S. Pershan, and J. O. Artman, Phys. Rev. **114**, 445 (1959).

¹⁰W. J. C. Grant, J. Phys. Chem. Solids **25**, 751 (1964).

¹¹T. Kohmoto, Y. Fukuda, M. Tanigawa, T. Mishina, and T. Hashi, Phys. Rev. B **28**, 2869 (1983).